THE JOURNAL OF BIOLOGICAL CHEMISTRY VOL. 280, NO. 42, pp. 35506–35512, October 21, 2005

Spontaneous Thermal Motion of the $GABA_A$ Receptor M2 Channel-lining Segments*

Received for publication, April 28, 2005, and in revised form, July 26, 2005 Published, JBC Papers in Press, August 9, 2005, DOI 10.1074/jbc.M504645200

Amal K. Bera[1] **and Myles H. Akabas**[2]

From the Departments of Physiology and Biophysics and of Neuroscience, Albert Einstein College of Medicine of Yeshiva University, Bronx, New York 10461

The γ-aminobutyric acid type A ($GABA_A$) receptor channel opening involves translational and rotational motions of the five channel-lining, M2 transmembrane segments. The M2 segment's extracellular half is loosely packed and undergoes significant thermal motion. To characterize the extent of the M2 segment's motion, we used disulfide trapping experiments between pairs of engineered cysteines. In $\alpha_1\beta_1\gamma_{2S}$ receptors the single γ subunit is flanked by an α and β subunit. The γ_2M2–14′ position is located in the α-γ subunit interface. $\gamma_2$13′ faces the channel lumen. We expressed either the $\gamma_2$14′ or the $\gamma_2$13′ cysteine substitution mutants with α_1 cysteine substitution mutants between 12′ and 16′ and wild-type β_1. Disulfide bonds formed spontaneously between $\gamma_2$14′C and both $\alpha_1$15′C and $\alpha_1$16′C and also between $\gamma_2$13′C and $\alpha_1$13′C. Oxidation by copper phenanthroline induced disulfide bond formation between $\gamma_2$14′C and $\alpha_1$13′C. Disulfide bond formation rates with $\gamma_2$14′C were similar in the presence and absence of GABA, although the rate with $\alpha_1$13′C was slower than with the other two positions. In a homology model based on the acetylcholine receptor structure, αM2 would need to rotate in opposite directions by ~80° to bring $\alpha_1$13′ and $\alpha_1$15′ into close proximity with $\gamma_2$14′. Alternatively, translational motion of αM2 would reduce the extent of rotational motion necessary to bring these two α subunit residues into close proximity with the $\gamma_2$14′ position. These experiments demonstrate that in the closed state the M2 segments undergo continuous spontaneous motion in the region near the extracellular end of the channel gate. Opening the gate may involve similar but concerted motions of the M2 segments.

Fast inhibitory neurotransmission in the central nervous system is largely mediated by the $GABA_A$[3] and glycine receptors (1). The receptors, members of the Cys loop gene superfamily of neurotransmitter-gated ion channels that includes nicotinic acetylcholine (ACh) and serotonin type 3 ($5\text{-}HT_3$) receptors (2–5), are formed by the assembly of five homologous subunits around the central channel axis. Each subunit has an ~200 amino acid extracellular N-terminal domain that forms the agonist binding sites and a similarly sized C-terminal domain with four α-helical, transmembrane segments (M1, M2, M3, and M4). For $GABA_A$ receptors formed by expression of α, β, and γ subunits, the most common subunit stoichiometry is two α subunits, two β subunits, and one γ subunit (6–8). Viewed from above, the subunits are arranged counterclockwise in the order βαγβα (9).

The $GABA_A$ receptor closed state structure is probably similar to the *Torpedo* ACh receptor structure that has been solved to 4-Å resolution (10–14). The ion channel is largely lined by the M2 transmembrane segments that form an inner ring of five α-helices. The inner ring of helices is surrounded by an outer ring of helices formed by the M1, M3, and M4 segments that separate the M2 segments from the lipid bilayer. In the 4-Å resolution ACh receptor structure, the extracellular halves of the M2 segments appear loosely packed, and the narrow region of the channel, inferred to be the channel gate, is between the 9′ and 14′[4] levels (14). This provides a static picture of the closed state.

Information on the dynamic protein motion in the membrane-spanning domain has been obtained using the substituted cysteine accessibility method (15, 16), disulfide trapping (17), and fluorescence (18). Substituted cysteine accessibility method studies of the β_1 subunit M2 segment in the presence of GABA showed a high degree of accessibility of the residues above 11′, suggesting loose packing and/or high mobility (19). In contrast, cysteine substituted at the cytoplasmic end of the channel between 2′ and 6′ had the limited accessibility consistent with that region of the channel being tightly packed with low mobility (10, 19). The cytoplasmic end of the channel contains the size and charge selectivity filters (10, 4). Disulfide trapping experiments between engineered Cys residues substituted for aligned M2 channel-lining residues at the 20′ level show that the M2 segments undergo translational motion across the channel lumen in the absence and the presence of GABA (20). In αβ receptors no disulfide bonds formed between Cys residues substituted for the 9′ and 13′ residues (17). In contrast, at the 6′ level we observed state-dependent disulfide bond formation in the presence of GABA, but not in its absence, between Cys residues in adjacent subunits. The 6′ disulfide bond formation significantly increased the channels' spontaneous open probability (17). We suggested that channel gating might involve a rotation of the M2 segments. Based on both the 9- and 4-Å resolution electron density maps of the ACh receptor, Unwin (14, 21) also suggested that the M2 segments may rotate during channel opening but to a much smaller extent. In voltage-dependent potassium channels it has been suggested that the S4 voltage sensor rotates, although other models have been proposed (22, 23).

Here we have used disulfide trapping experiments to probe the spontaneous thermal motion of the M2 segments for evidence of rotational motion. The ability of a pair of Cys residues to form a disulfide bond depends on the presence of an oxidizing environment and on the pair's collision frequency. The collision frequency depends on the average

* This work was supported in part by National Institutes of Health Grants NS30808 and GM61925 (to M. H. A.). The costs of publication of this article were defrayed in part by the payment of page charges. This article must therefore be hereby marked "*advertisement*" in accordance with 18 U.S.C. Section 1734 solely to indicate this fact.

[1] Present address: Dept. of Biotechnology, Indian Inst. of Technology Madras, Chennai 600 036, India.

[2] To whom correspondence should be addressed: Dept. of Physiology and Biophysics, Albert Einstein College of Medicine, 1300 Morris Park Ave., Bronx, NY 10461. Tel.: 718-430-3360; Fax: 718-430-8819; E-mail: makabas@aecom.yu.edu.

[3] The abbreviations used are: $GABA_A$, γ-aminobutyric acid type A; ACh, acetylcholine; CFFR, Ca^{2+}-free frog Ringers solution; Cu:phen, copper phenanthroline; DTT, dithiothreitol.

[4] Positions in the M2 segment are identified by a system of index numbers to facilitate comparison between Cys loop receptors (37). In this system the absolutely conserved basic residue at the N-terminal end of M2 is numbered 0′. Residues toward the C-terminus are numbered 1′, 2′, 3′, etc. Residues toward the N-terminus are numbered −1′, −2′, etc. For the 0′, residues are $GABA_A$ receptors α_1R255, β_1R250, and γ_2R265.

separation distance between the sulfhydryls, their relative orientation in the protein, and the protein's flexibility/mobility in the region of the Cys residues. We used copper phenanthroline (Cu:phen) to create an oxidizing environment. Cu:phen catalyzes the formation of reactive oxygen species such as superoxide and hydroxyl radicals from molecular oxygen (24). Spontaneous disulfide bond formation indicates that mildly oxidizing conditions due to ambient oxygen in our buffer were sufficient to promote disulfide bond formation. This is not fundamentally different from disulfide bond formation in the more oxidizing environment created by Cu:phen. Spontaneous disulfide bond formation as compared with Cu:phen-induced formation is simply a measure of the relative propensity to form disulfide bonds. For a disulfide bond to form, the Cys α carbons must come to within 5.6 Å of one another (25). It is important to recognize that formation of a disulfide bond does not imply that the time average separation of the two α carbons is 5.6 Å. One can infer that in the course of thermal motion the cysteines can approach to within this distance. Disulfide trapping has been used to study protein mobility and proximity relationships between residues in both water-soluble and integral membrane proteins (25–29).

For these experiments we took advantage of the fact that in $\alpha\beta\gamma$ receptors there is a single γ-α subunit interface. Based on our earlier substituted cysteine accessibility method experiments in the α subunit we predicted that the γ_2M2 14′ residue lies in the α-γ subunit interface (10). We probed the ability of a Cys substituted for $\gamma_2$14′ to form disulfide bonds with Cys substituted for $\alpha_1$12′ to $\alpha_1$16′ residues in the absence of GABA. We hypothesized that if disulfide bonds could form between $\gamma_2$14′ and multiple sites on the αM2 segment, it would suggest that αM2 was moving relative to the $\gamma_2$14′ position. Our data demonstrate that γ14′C formed disulfide bonds with multiple α-substituted Cys residues that are separated by ~160° on the circumference of the α helix. We also probed the ability of $\gamma_2$13′C to form disulfide bonds with $\alpha_1$11′C to $\alpha_1$13′C. The $\gamma_2$13′C formed a disulfide bond with $\alpha_1$13′C.

MATERIALS AND METHODS

Mutagenesis and Oocyte Expression—All cysteine substitution mutants were made using PCR as described previously (19). mRNA was synthesized in vitro using the AmpliCap T7 high yield message maker kit (Epicenter Technologies, Madison, WI). mRNA was dissolved in diethylpyrocarbamate-treated water and stored at −80 °C. *Xenopus laevis* specimens were purchased from Nasco Science (Fort Atkinson, WI). Stage V-VI oocytes were defolliculated by incubation in 2 mg/ml type 1A collagenase (Sigma) for 75 min. Oocytes were washed in OR2 (82.5 mM NaCl, 2 mM KCl, 1 mM $MgCl_2$, and 5 mM HEPES; pH adjusted to 7.5 with NaOH) and kept in OR3 (70% Leibovitz's L-15 medium (Invitrogen) supplemented with 10 mM HEPES, 50 μg/ml tetracycline, and 50 μg/ml gentamicin). Oocytes were injected 24 h after isolation with 50 nl of a 1:1:1 mixture of rat $\alpha_1/\beta_1/\gamma_{2S}$ subunit mRNA (200 pg/nl) and kept in OR3 medium for 2–5 days at 17 °C.

Reagents—A 100 mM stock solution of GABA (Sigma) in water was aliquoted and stored at −20 °C. 1 M stock solutions of dithiothreitol (DTT; Sigma) and *o*-phenanthroline (Sigma) were made in nominally calcium-free frog Ringer's solution (CFFR; 115 mM NaCl, 2.5 mM KCl, 1.8 mM $MgCl_2$, and 10 mM HEPES, pH 7.5) and dimethyl sulfoxide, respectively, aliquoted, and stored for not more than one month at −20 °C. A stock solution of 100 mM $CuSO_4$ was made in water. $CuSO_4$ and *o*-phenanthroline were mixed in CFFR directly before use to a final concentration of 100 μM $CuSO_4$ and 200 μM *o*-phenanthroline expressed as 100:200 μM Cu:phen.

Electrophysiology—Two electrode voltage clamp recordings were conducted at room temperature in a 250-μl chamber continuously perfused at 5–6 ml/min with CFFR solution at a holding potential of −60 mV. The ground electrode was connected to the bath via a 3 M KCl/agar bridge. Glass microelectrodes filled with 3 M KCl had a resistance of <2 megaohms. Data were acquired and analyzed using a TEV-200 amplifier (Dagan Instruments, Minneapolis, MN), a Digidata 1322A data interface (Axon Instruments, Union City, CA), and pClamp 8 software (Axon Instruments). Currents were elicited by applications of GABA separated by at least 5 min of CFFR wash to allow complete recovery from desensitization. Currents were judged to be stable if the variation between consecutive GABA pulses was <5%.

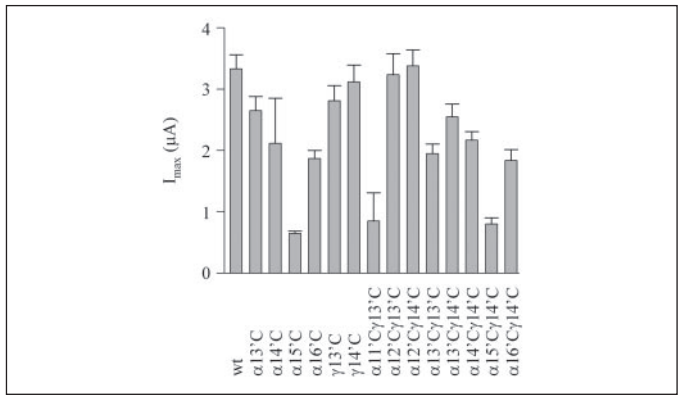

FIGURE 1. **GABA-induced maximal currents (I_{max}) of wild type (*wt*) and mutant receptors formed by coexpression of α_1, β_1, and γ_2 subunits.** Only subunits containing an engineered cysteine are shown.

Disulfide Bond-induced Inhibition—Once GABA-induced control currents had stabilized, 10 mM DTT was applied for 3 min. GABA was reapplied directly following DTT to determine the extent of potentiation produced by the reduction of spontaneously formed disulfide bonds. The cells were treated with 100:200 μM Cu:phen for 1 min, and then two or more GABA test pulses were applied.

DTT can both reduce a disulfide bond and bind Cu^{2+} with high affinity. To confirm that the ability of DTT to reverse the effects of Cu:phen was due to disulfide bond formation and not to Cu^{2+} chelation by one or both of the engineered Cys residues, we assayed the effect of a 1-min application of 1 mM EGTA. EGTA chelates Cu^{2+} with high affinity but cannot reduce a disulfide bond. If EGTA failed to reverse the effect of Cu:phen, a second application of 10 mM DTT (3 min) was followed by a final test pulse of GABA to demonstrate that DTT was able to reverse the effect of Cu:phen.

The extent of potentiation attributed to the reduction of spontaneously formed disulfide bonds was calculated by the equation percentage effect = $[(I_{DTT} - I)/I]\cdot 100$, where I_{DTT} is the GABA-induced current following application of DTT and I is the current prior to DTT treatment. The effect of Cu:phen was calculated in a similar way except that I is the GABA current after Cu:phen. 500 μM GABA was used for all experiments except where specified. The maximal currents and percentage effect for each reagent are presented as the mean ± S.E.

Reoxidation Rates—A test pulse of 500 μM GABA was followed by a 3-min application of 10 mM DTT and a test pulse of GABA. The current magnitude of the second test pulse was significantly larger than the GABA current before DTT. Cu:phen (50:100 μM) with or without saturating GABA was applied for 3 s. After a 5-min wash with CFFR, a GABA test pulse was applied, and the peak current was measured. The brief pulses of Cu:phen alternating with GABA test pulses continued until the GABA test pulse current magnitude reached a plateau. The durations of the Cu:phen applications varied between 3 and 40 s depending on the extent of inhibition caused by the previous pulse. As the GABA test currents reached the plateau, longer Cu:phen applica-

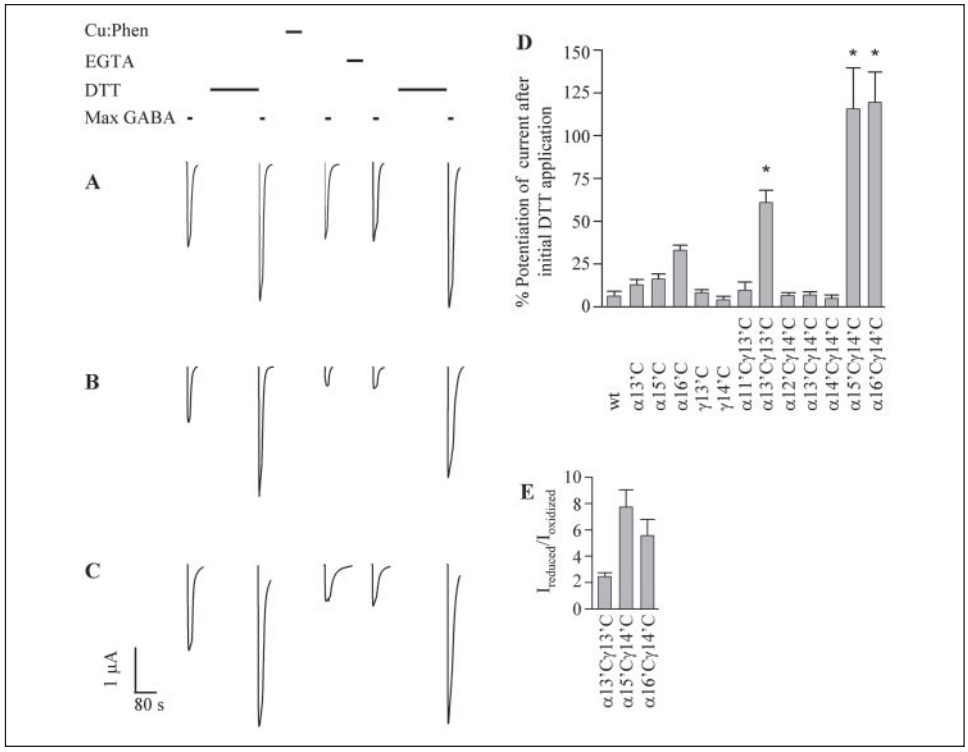

FIGURE 2. **Spontaneous and Cu:phen-induced disulfide bond formation between different cysteine pairs.** *A–C*, effects of DTT and Cu:phen on the GABA-induced currents of oocytes expressing the mutants $\alpha_1 13\beta_1\gamma_2 13'C$ (*A*), $\alpha_1 15'C\beta_1\gamma_2 14'C$ (*B*), and $\alpha_1 16'C\beta_1\gamma_2 14'C$ (*C*). *Bars* at the *top* apply to all three panels and indicate the period of application of the reagent listed on the *left*. The first application of DTT increased the GABA-induced currents for all three mutants, indicating the presence of spontaneously formed disulfide bonds. A subsequent application of Cu:phen diminished the currents. EGTA application did not reverse the Cu:phen effect, but DTT application did reverse the Cu:phen effect. For the mutants $\alpha_1 15'C\beta_1\gamma_2 14'C$ and $\alpha_1 16'C\beta_1\gamma_2 14'C$ (*panels B* and *C*, respectively), Cu:phen decreased the currents to a level below the initial currents, indicating that not all receptors had spontaneously formed disulfide bonds. *D*, the effect of the first DTT application on GABA currents. Depicted is the percentage potentiation of initial I_{max} by DTT for all mutants. Double mutants were compared with the corresponding single α and γ mutants by one-way analysis of variance with the Newman-Keul's post hoc test. An *asterisk* (*) *over* the *bars* indicate a statistically significant difference ($p < 0.001$) for the corresponding single mutants. *E*, ratio of the I_{max} of fully reduced channels (after DTT) to that of fully oxidized channels (after Cu:phen) for three of the mutants shown in *panels A*, *B*, and *C*.

tions were made to demonstrate that the reaction had gone to completion. The magnitude of GABA-induced test pulse currents was normalized relative to the current induced by GABA test pulses after the application of DTT. The normalized currents were plotted as a function of cumulative exposure time to the Cu:phen and fitted with the equation $I_t = (I_0 - I_\infty)\exp(-t/\tau) + I_\infty$, where I_t is the current at time t, I_0 is the initial current, I_∞ is the final current, and τ is the time at which 63% of the total current decay occurred.

Statistics—All statistical analyses were performed in Prism 3.02 using a one-way analysis of variance followed by the Newman-Keuls multiple comparison test. All data are presented as the mean ± S.E.

RESULTS

Characterization of the Individual Cysteine Mutants—Oocytes expressing each of the individual α_1 subunit Cys-substitution mutants $\alpha_1 12'C$, $\alpha_1 13'C$, $\alpha_1 14'C$, $\alpha_1 15'C$, and $\alpha_1 16'C$, when co-expressed with wild-type β_1 and γ_2, displayed GABA-activated currents (Fig. 1). The currents of $\alpha_1 15'C\beta_1\gamma_2$ were significantly smaller than those of the other mutants but were nevertheless sufficiently large for the purposes of these experiments.

Application of 10 mM DTT for 3 min had no effect on the subsequent GABA-induced currents of any of the single α_1 Cys mutants (Fig. 2*D*). We infer that none of the α_1 Cys mutants formed spontaneous disulfide bonds between the two α-engineered Cys residues within a receptor or between the engineered Cys residues and the endogenous Cys residues. Oocytes expressing either of the two γ_2 Cys mutants used in this study, $\gamma_2 13'C$ or $\gamma_2 14'C$, with wild type α_1 and β_1 subunits also displayed GABA-induced currents and were unaffected by a 3-min application of 10 mM DTT (Figs. 1 and 2*D*).

Oxidation by a 1-min application of 100:200 μM Cu:phen to oocytes expressing $\alpha\beta\gamma$ receptors with one of the Cys substitution mutants had no effect on the subsequent GABA-induced currents (Fig. 3*B*). We infer that none of the individual α_1 or γ_2 Cys mutants formed disulfide bonds with either the engineered or the endogenous Cys residues.

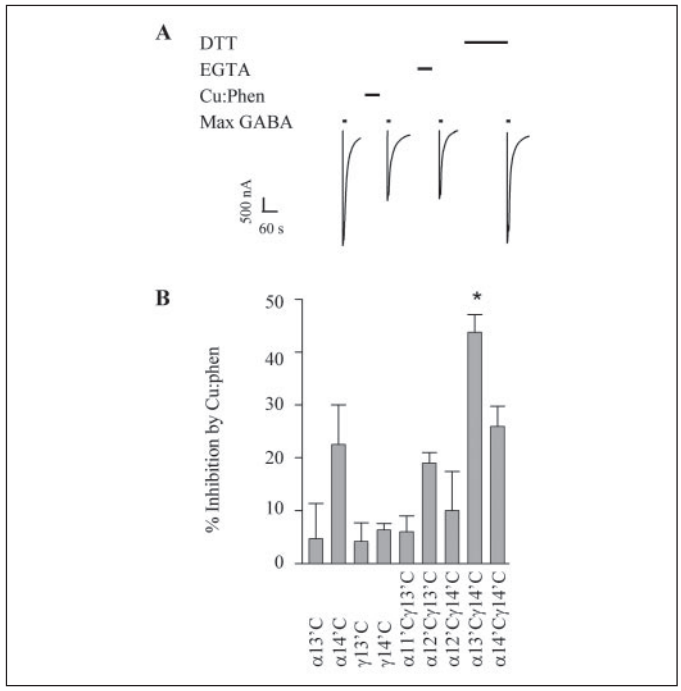

FIGURE 3. **Effect of Cu:phen-induced oxidation of Cys mutants that did not form spontaneous disulfide bonds.** Cu:phen induced disulfide bond formation between $\alpha_1 13'C$ and $\gamma_2 14'C$. *A*, Cu:phen reduced the I_{max} of the mutant $\alpha_1 13'C\beta_1\gamma_2 14'C$. The effects of Cu:phen were reversed by DTT but not by EGTA. *B*, the percentage inhibition of I_{max} by Cu:phen for mutants that did not spontaneously form disulfide bonds. Cu:phen significantly reduced the I_{max} of the double mutant $\alpha_1 13'C\beta_1\gamma_2 14'C$ ($p < 0.001$, by one-way analysis of variance with the Newman-Keuls post hoc test) in comparison to either of the single mutants $\alpha_1 13'C$ or $\gamma_2 14'C$.

Spontaneous Disulfide Bond Formation between Pairs of Cysteine Mutants—Oocytes expressing each of the individual α_1 Cys mutants with $\gamma_2 14'C$ and wild type β_1 displayed GABA-induced currents (Figs. 1 and 2). For two of the double Cys mutants, $\alpha_1 15'C\beta_{1\gamma_2} 14'C$ and

$\alpha_1$16′C$\beta_{1\gamma2}$14′C, a 3-min application of 10 mM DTT significantly increased the subsequent GABA-induced currents (Fig. 2). The increase in GABA-induced current was reversed by a 1-min application of the oxidizing reagent Cu:phen (100:200 μM). A subsequent application of 10 mM DTT for 3 min restored the GABA-induced currents to a level similar to the level after the first application of DTT (Fig. 2*E*). We infer that for these two double mutants a disulfide bond had formed spontaneously prior to the start of the experiment. The disulfide bond could be reduced by DTT and reformed by oxidation with Cu:phen. The ability to reverse the Cu:phen effect with DTT indicated that the Cu:phen effect was due to disulfide bond formation and not because of the oxidation of the engineered Cys to higher order oxidation states.

A disulfide bond also formed spontaneously between $\gamma_2$13′C and $\alpha_1$13′C when the mutants were expressed in $\alpha\beta\gamma$ receptors. An initial application of 10 mM DTT (3 min) caused a significant increase in subsequent GABA-induced currents (Fig. 2*D*). This increase was reversed by Cu:phen application in a manner similar to that described above (Fig. 2*E*).

To rule out the possibility that the inhibition caused by the Cu:phen application might due to Cu^{2+} binding by the engineered Cys, we applied 1 mM EGTA for 1 min. This had no effect on the GABA-induced currents (Fig. 2).

Cu:Phen-induced Disulfide Bond Formation.—For the $\alpha_1$12′C, $\alpha_1$13′C, and $\alpha_1$14′C that did not spontaneously form disulfide bonds with $\gamma_2$14′C, we tested whether disulfide bond formation could be induced in the more oxidizing environment created by Cu:phen application. A 1-min application of 100:200 μM Cu:phen to oocytes expressing $\alpha_1$13′C$\beta_{1\gamma2}$14′C caused a significant inhibition (43% ± 3; n = 11) of the subsequent GABA-induced currents (Fig. 3). This inhibition was not reversed by a 1-min application of 1 mM EGTA but was reversed by a 3-min application of 10 mM DTT (Fig. 3*A*). We inferred that a disulfide bond could be formed between the $\alpha_1$13′- and $\gamma_2$14′-engineered Cys. A similar application of Cu:phen to oocytes expressing either $\alpha_1$12′C$\beta_{1\gamma2}$14′C or $\alpha_1$14′C$\beta_{1\gamma2}$14′C had no effect on subsequent GABA currents. This finding implies that no disulfide bonds could be induced in these double mutants.

Time Constants for Cu:Phen-induced Disulfide Bond Formation.—We compared the time constants for Cu:phen-induced disulfide bond formation between $\gamma_2$14′C and the three α_1 Cys mutants, 13′, 15′ and 16′, with which it formed disulfide bonds. Actual rate constants were not determined because the concentration of the reactants is unknown, but rather the time constant for the decay of GABA-induced currents due to disulfide bond formation was determined. The time constants were calculated by determining the effects of repeated brief (3–40 s) applications of 50:100 μM Cu:phen on the GABA-induced test currents as illustrated in Fig. 4*A*. The resultant GABA-induced currents were normalized by the initial GABA current and plotted as a function of cumulative Cu:phen application time and fitted with a single exponential decay function (Fig. 4*B*). The time constants for disulfide bond formation in the absence of GABA between $\gamma_2$14′C and both $\alpha_1$15′C and $\alpha_1$16′C were similar, ~5 s (TABLE ONE). The time constant for disulfide bond formation between $\gamma_2$14′C and $\alpha_1$13′C was larger, ~9 s, than that for the other two pairs (TABLE ONE). This slower time constant is consistent with the lack of spontaneous disulfide bond formation between this pair of Cys mutants, which suggests that the collision frequency is lower between this pair of Cys mutants. The time constants of Cu:phen-induced disulfide bond formation were also measured in the presence of GABA. The time constants with the $\gamma_2$14′C were unaffected by the presence of GABA.

The time constant for disulfide bond formation between the aligned 13′ positions, $\gamma_2$13′C and $\alpha_1$13′C, was slower than that for the disulfide bonds formed with $\gamma_2$14′C. For this 13′ pair of residues the time constant increased 3-fold in the presence of GABA (TABLE ONE). We do not know whether disulfide bond formation in the presence of GABA is occurring in the open or the desensitized states.

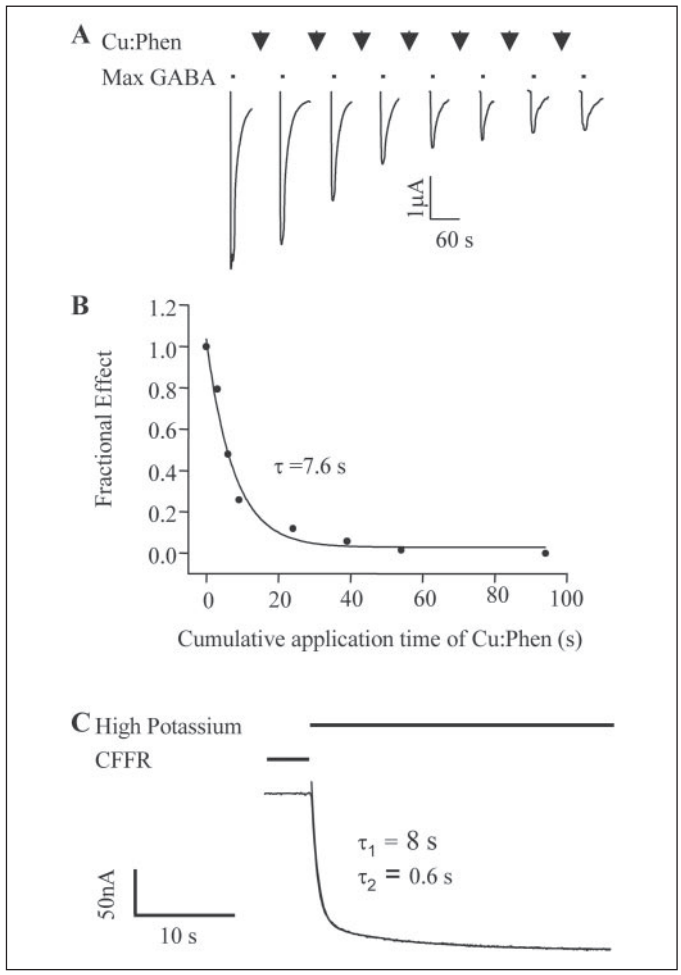

FIGURE 4. **Measurement of the time constant for disulfide bond formation between $\alpha_1$16′C and $\gamma_2$14′C.** *A, traces* produced by pulses of 500 μM GABA in the $\alpha_1$16′C$\beta_1\gamma_2$14′C mutant are shown. At each *downward arrow*, 50:100 μM of Cu:phen was applied briefly. The duration of the first three applications was 3 s each, the next 3 applications were 15 s each, and the final application was 40 s to demonstrate that reaction had gone to completion. Each application of GABA was followed by a 5–7 min wash with CFFR. *B*, normalized currents from *panel A* were plotted against cumulative application time of Cu:phen and fitted with a single exponential decay function. τ, 7.6 s in this experiment, was calculated as 1/k, where k is the decay constant. *C*, current trace recorded from an uninjected oocyte clamped at −80 mV. Currents developed as the perfusion buffer was switched from CFFR to high potassium buffer. The current trace was fitted with a double exponential decay function with two τs, namely τ_{fast} = 0.6 s (0.66 ± 0.14 s, n = 5) and τ_{slow} = 8 s (7.5 ± 1.2 s, n = 5). In the experiment shown, the τ_{fast} contributes 81% of the total currents, where as τ_{slow} contributes only 19%. The major component of the solution exchange took place on a time scale 10 times faster than the time constant of the disulfide bond formation. Thus, solution exchange did not limit the measurement of disulfide bond formation time constants.

To ensure that the measured time constants were not limited by our solution exchange rates, we measured the time constant of the change in the resting membrane current as we switched the perfusion solution from CFFR to a high potassium solution (115 mM KCl, 2.5 mM NaCl, 1.8 mM $MgCl_2$, and 10 mM HEPES, pH 7.5). The current change in response to the switch from CFFR to high K^+ solution was best fit with a double exponential equation (Fig. 4*C*). The fast time constant (0.6 ± 0.1 s, n = 5) accounted for 75 ± 6% of the current change. The slow time constant (7.5 ± 1.2 s, n = 5) accounted for only 25% of the current change. The major component of the solution exchange took place on a time scale 10 times faster than the time constant of the disulfide bond formation. Thus, solution exchange rates did not limit the measurement of the disulfide bond formation time constants.

TABLE ONE

Time constants (τ) for disulfide bond formation between different cysteine pairs

Mutant	Cu:phen (τ)	n[a]	Cu:phen + GABA (τ)	n[a]	Cα separation distance
	s		*s*		*Å*
α13′Cγ13′C	15 ± 2[b]	3	5 ± 0.7[c]	4	8.4[d]
α13′Cγ14′C	9 ± 3	4	11 ± 3	3	6.6
α15′Cγ14′C	5 ± 1	5	5 ± 2	3	10.4
α16′Cγ14′C	6 ± 1	4	4 ± 1	4	7.7

[a] Number of oocytes.
[b] Time constant is significantly different from mutants α15′Cγ14′C and α16′Cγ14′C ($p < 0.05$).
[c] Significant difference between time constants in the presence and absence of GABA ($p < 0.05$).
[d] Cα-Cα separation distance for respective positions measured from the 2BG9 atomic coordinates.

DISCUSSION

GABA$_A$ receptor channel gating involves conformational change in the M2 channel-lining segments in order to open the channel gate (10, 4, 14). The 4-Å resolution structure of the homologous ACh receptor provides a static view of the closed state structure but little insight into the mobility of the protein. In the region of the 20′ position, the M2 segments undergo significant spontaneous thermal motion, but the extent of this motion deeper in the channel and the nature of the motion, rotation or translation or both, is unknown (17, 20). In the present work we have probed the extent of spontaneous thermal motion between engineered Cys residues on the M2 segments of adjacent subunits at the extracellular end of the putative channel gate (14) using disulfide trapping. These experiments showed that disulfide bonds formed spontaneously between a Cys at $\gamma_2$14′ and a Cys at either the $\alpha_1$15′ or the $\alpha_1$16′ position. The disulfide bond formation rates were similar for these two γ-α Cys pairs. This result suggests that the relative collision frequency between the $\gamma_2$14′C and the $\alpha_1$15′ and $\alpha_1$16′ positions were similar. In a more oxidizing environment created by the presence of copper phenanthroline, a disulfide bond was also formed between $\gamma_2$14′C and $\alpha_1$13′C. The disulfide bond formation rate was significantly slower between these two residues than between the other two γ-α Cys pairs, suggesting that the collision frequency between $\gamma_2$14′ and the $\alpha_1$13′ position is lower than that with the other two αM2 positions.

In contrast to the disulfide bonds formed by γ14′C, the disulfide bond formation rate for the bond formed between γ13′C and α13′C was significantly faster in the presence of GABA compared with that in the absence of GABA. In the presence of GABA the channels undergo transitions between the open and desensitized states. We cannot distinguish in which state disulfide bond formation is occurring. We can infer, however, that the collision frequency between aligned positions at the 13′ level is greater in the presence of GABA.

The extent of the motion of one M2 segment relative to the adjacent M2 segment can be estimated from the separation distances of the aligned positions in the 4-Å resolution structure of the homologous ACh receptor (14). In a disulfide bond, the center-to-center distance separating the sulfurs is 2 Å, and that separating the α carbons is ~5.6 Å (30, 25). In the ACh receptor structure (Protein Data Bank code 2BG9) the α carbon separation between the positions aligned with γ14′ and α15′ and α16′ is ~10 and ~8 Å, respectively (measured from the protein data bank 2BG9 atomic coordinate file). The separation between $\gamma_2$14′ and $\alpha_1$13′ is ~7 Å. The sulfur-sulfur separation distances are dependent on the specific side chain rotamer used and can vary by 2 to 3 Å. Thus, distance alone does not determine the likelihood of disulfide bond formation, suggesting that certain motions are constrained by the protein structure. This was observed previously in the aspartate chemotaxis receptor (25).

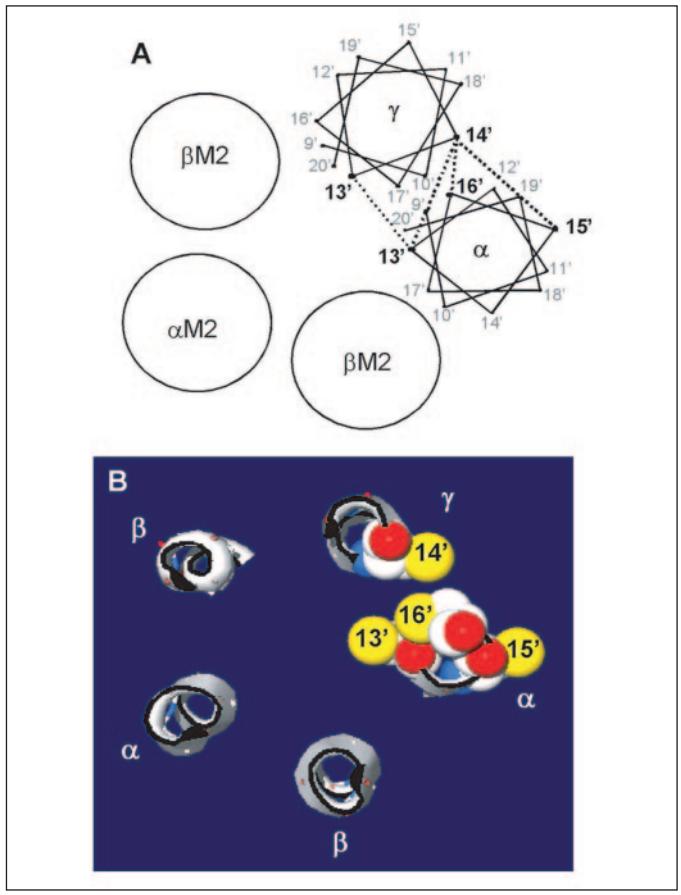

FIGURE 5. **Cross-sectional views of the M2 segments lining the GABA$_A$ receptor channel.** *A*, α-helical wheel representation of M2 segments (from 10′ to 19′) of the α and γ subunits. Broken lines represent the disulfide bond between two engineered cysteines. The positions of engineered cysteines that form disulfide bonds are shown in a big *black square*. All disulfide bonds except those between $\alpha_1$13′C and $\gamma_2$14′C formed spontaneously. *B*, slab view through the M2 segments from 11′ to 16′ levels, looking down from the extracellular space based on the ACh receptor 2BG9 Protein Data Bank coordinates. For $\gamma_2$14′, $\alpha_1$13′, $\alpha_1$15′, and $\alpha_1$16′, the native side chain has been mutated to cysteine using DeepView (Swiss-PdbViewer version 3.7) and rendered using POV-Ray version 3.5. The van der Waals surfaces are only shown for the cysteines (*yellow*, sulfur; *red*, oxygen; *blue*, nitrogen; *white*, carbon). Side chains of other residues are not shown. The backbone is in *white ribbon* representation.

On the circumference of an α helix the 15′ and 16′ positions are separated by an arc of 100°, whereas the 15′ and 13′ positions are separated by an arc of 160°. A rotational motion of the αM2 segment could move these residues into close proximity with γ14′. This would require the αM2 segment to rotate on its helix axis from its position in the 4-Å structure ~80° in one direction for α15′ and 80° in the opposite direction for α13′ (Fig. 5). Looking from the extracellular side down the M2

helix, the counter-clockwise rotation that would bring $\alpha_1 15'$ into close proximity with $\gamma_2 14'$ is more likely than the clockwise rotation that would bring $\alpha_1 13'$ into close proximity. Consistent with the M2 segments undergoing significant rotational motion, we showed previously that a disulfide bond could form between Cys residues substituted at the channel-lining 6′ position in adjacent subunits (17). At the 6′ level the disulfide bond involved the non-GABA binding subunit. In order for aligned positions on adjacent M2 segments to come into close proximity, the M2 segments must rotate asymmetrically either in time, one before the next, or in space, toward each other. There are precedents for helix rotation in proteins, including the aspartate chemotaxis receptor (25), voltage-dependent K^+ channels (22), cyclic nucleotide-gated channels (31), bacteriorhodopsin (32), and the mitochondrial ADP/ATP carrier (33). However, we are concerned that the large rotation required to bring the $\alpha 13'$ and $\alpha 15'$ seems significantly larger than what is reasonable to expect for normal motion within a protein.

Alternatively, a combination of translational and rotational motion of the M2 segment would reduce the amount of rotational motion necessary to bring the $\gamma_2 14'$ and $\alpha_1 13'$, $\alpha_1 15'$, and $\alpha_1 16'$ positions into close proximity (Fig. 5). A sweeping motion of the M2 segment as it translates away from the central channel axis outward toward the outer ring of helices could produce a rotation around an axis other than the helix axis. Such a motion has been proposed for ACh receptor gating (13, 14). Recently, we and others have suggested that the cytoplasmic end of the M2 segment, in the vicinity of the 2′ position, is relatively tightly packed and undergoes little conformational change during gating (19, 34). The extracellular end of the M2 segments may move outward during channel gating, away from the channel axis, whereas the cytoplasmic end could act as a relatively fixed fulcrum. This would open the narrow region of the channel between the 9′ and 14′ positions (13, 14). All of the disulfide bonds between $\gamma_2 14'$ and $\alpha_1 13'$, $\alpha_1 15'$, and $\alpha_1 16'$ formed in the absence of agonist, presumably in the closed resting state of the channel. Thus, even in the resting state the channel-lining M2 segments at the level of the upper end of the putative channel gate are undergoing significant thermal motion. Perhaps in the closed state the M2 segments are spontaneously undergoing a sweeping/rotational motion between their closed and open state conformations, similar to the motion that occurs during channel gating but in a non-concerted fashion. Thus, in the absence of an agonist it is extremely unlikely at any given time that all of the M2 segments would be in the open state position (*i.e.* spontaneous opening is a very rare event); however, individual M2 segments are constantly but transiently moving into the open state position, resulting in relative motion of adjacent M2 segments in the resting state of the channel.

The conformational motion in the channel-lining M2 segments in the closed state may be important for the function of the protein. The channel must open rapidly (35) and with an energy barrier between the closed and open state comparable with the binding energy of two GABA molecules. Thus, if the M2 segments were tightly packed with extensive contacts, the ability to open the channel might be limited. In crystal structures of other proteins it has been shown that the flexibility of a region is inversely proportional to the extent of protein contacts between that region and the rest of the protein (36). Thus, the flexibility that is necessary for rapid gating of $GABA_A$ receptor channels may require that in the closed state the extent of protein contact between the M2 segments be limited, thus allowing the dynamic motion that we have documented in the present work and previously (19, 20).

It is notable that the disulfide bond formation rates between $\gamma_2 14'$ and $\alpha_1 13'$, $\alpha_1 15'$, and $\alpha_1 16'$ were similar in both the absence and the presence of GABA. In the prolonged presence of GABA (~1 min), most of the channels are in the desensitized state. Thus, the similarity of the disulfide bond formation rates may indicate that the dynamic motion of the M2 segments is similar in the closed and desensitized states. The fraction of time spent in the open state may not be sufficient to change the reaction rate. In contrast, the disulfide bond between $\gamma 13'$ and $\alpha 13'$ formed three times faster in the presence of GABA. At the 20′ level, the disulfide bond formation rate was also about three times faster in the presence of GABA (17). At present it is unclear why in the same region of the channel the reaction rates for some residues should be similar in both the absence and the presence of GABA, whereas between other pairs of residues the rates should be accelerated in the presence of GABA. This finding suggests that although the extent of thermal motion of the M2 segments in the closed and desensitized states may be similar, the channel structure of these two states may be somewhat different. Regarding the $\gamma_2 13'C$ to $\alpha_1 13'C$ disulfide bond, we do not know that it is forming between the adjacent subunits. It might be forming between the non-adjacent α subunit and the γ subunit because these are channel-lining residues (10, 19). In addition, we cannot determine whether, in the presence of GABA, this disulfide is forming in the open or desensitized states.

Although the Cα-Cα separation distance between $\gamma_2 14'C$ and $\alpha_1 12'C$ is 8.7 Å, within the range of residues that formed disulfide bonds with $\gamma_2 14'C$ (TABLE ONE and Fig. 5) we saw no evidence of disulfide bond formation between these engineered cysteine residues. Negative results must be interpreted with care. Disulfide trapping identifies pairs of positions that allow the sulfur atoms in the engineered cysteines to collide with sufficient frequency and energy to allow disulfide bond formation to occur. There are many factors that might prevent a specific pair from colliding with sufficient frequency or in the appropriate orientation to allow measurable rates of disulfide bond formation.

In summary, these and previous experiments indicate that the channel-lining M2 segments between the 13′ and 20′ levels undergo continuous spontaneous motion in the closed state. The structure is quite dynamic. This motion appears to involve both rotational and translational components. These movements may be related to the conformational changes that the subunits undergo during channel opening that may involve the rotation of the M2 segments as well as their translation away from the channel axis. The extent of thermal motion is consistent with the loose packing of the extracellular halves of the M2 segments observed in the cryoelectron microscopic structure of the homologous ACh receptor (36). Further studies will help to define the specific conformational changes involved in opening the channel gate.

Acknowledgments—We thank Rachel Berkowitz for technical assistance and Moez Bali, Jeffrey Horenstein, Michaela Jansen David Liebelt, Nicole McKinnon, David Reeves, and Paul Riegelhaupt for helpful discussions and also for comments on this manuscript.

REFERENCES

1. Rabow, L. E., Russek, S. J., and Farb, D. H. (1995) *Synapse* **21,** 189–274
2. Karlin, A. (2002) *Nat. Rev. Neurosci.* **3,** 102–114
3. Reeves, D. C., and Lummis, S. C. (2002) *Mol. Membr. Biol.* **19,** 11–26
4. Lester, H. A., Dibas, M. I., Dahan, D. S., Leite, J. F., and Dougherty, D. A. (2004) *Trends Neurosci.* **27,** 329–336
5. Olsen, R. W., Chang, C. S., Li, G., Hanchar, H. J., and Wallner, M. (2004) *Biochem. Pharmacol.* **68,** 1675–1684
6. Chang, Y., Wang, R., Barot, S., and Weiss, D. S. (1996) *J. Neurosci.* **16,** 5415–5424
7. Tretter, V., Ehya, N., Fuchs, K., and Sieghart, W. (1997) *J. Neurosci.* **17,** 2728–2737
8. Baumann, S. W., Baur, R., and Sigel, E. (2001) *J. Biol. Chem.* **276,** 36275–36280
9. Brejc, K., van Dijk, W. J., Klaassen, R. V., Schuurmans, M., van Der Oost, J., Smit, A. B., and Sixma, T. K. (2001) *Nature* **411,** 269–276
10. Xu, M., and Akabas, M. H. (1996) *J. Gen. Physiol.* **107,** 195–205
11. Teissere, J. A., and Czajkowski, C. (2001) *J. Neurosci.* **21,** 4977–4986

12. Cromer, B. A., Morton, C. J., and Parker, M. W. (2002) *Trends Biochem. Sci.* **27,** 280–287
13. Miyazawa, A., Fujiyoshi, Y., and Unwin, N. (2003) *Nature* **423,** 949–955
14. Unwin, N. (2005) *J. Mol. Biol.* **346,** 967–989
15. Akabas, M. H., Stauffer, D. A., Xu, M., and Karlin, A. (1992) *Science* **258,** 307–310
16. Xu, M., and Akabas, M. H. (1993) *J. Biol. Chem.* **268,** 21505–21508
17. Horenstein, J., Wagner, D. A., Czajkowski, C., and Akabas, M. H. (2001) *Nat. Neurosci.* **4,** 477–485
18. Dahan, D. S., Dibas, M. I., Petersson, E. J., Auyeung, V. C., Chanda, B., Bezanilla, F., Dougherty, D. A., and Lester, H. A. (2004) *Proc. Natl. Acad. Sci. U. S. A.* **101,** 10195–10200
19. Goren, E. N., Reeves, D. C., and Akabas, M. H. (2004) *J. Biol. Chem.* **279,** 11198–11205
20. Horenstein, J., Riegelhaupt, P., and Akabas, M. H. (2005) *J. Biol. Chem.* **280,** 1573–1581
21. Unwin, N. (1995) *Nature* **373,** 37–43
22. Cha, A., Snyder, G. E., Selvin, P. R., and Bezanilla, F. (1999) *Nature* **402,** 809–813
23. Jiang, Y., Lee, A., Chen, J., Ruta, V., Cadene, M., Chait, B. T., and MacKinnon, R. (2003) *Nature* **423,** 33–41
24. Kobashi, K. (1968) *Biochim. Biophys. Acta* **158,** 239–245
25. Careaga, C. L., and Falke, J. J. (1992) *J. Mol. Biol.* **226,** 1219–1235
26. Regan, L., Rockwell, A., Wasserman, Z., and DeGrado, W. (1994) *Protein Sci.* **3,** 2419–2427
27. Yu, H., Kono, M., McKee, T. D., and Oprian, D. D. (1995) *Biochemistry* **34,** 14963–14969
28. Wu, J., and Kaback, H. R. (1996) *Proc. Natl. Acad. Sci. U. S. A.* **93,** 14498–14502
29. Hastrup, H., Karlin, A., and Javitch, J. A. (2001) *Proc. Natl. Acad. Sci. U. S. A.* **98,** 10055–10060
30. Sowdhamini, R., Srinivasan, N., Shoichet, B., Santi, D. V., Ramakrishnan, C., and Balaram, P. (1989) *Protein Eng.* **3,** 95–103
31. Johnson, J. P., Jr., and Zagotta, W. N. (2001) *Nature* **412,** 917–921
32. Xiao, W., Brown, L. S., Needleman, R., Lanyi, J. K., and Shin, Y. K. (2000) *J. Mol. Biol.* **304,** 715–721
33. Kihira, Y., Iwahashi, A., Majima, E., Terada, H., and Shinohara, Y. (2004) *Biochemistry* **43,** 15204–15209
34. Panicker, S., Cruz, H., Arrabit, C., Suen, K. F., and Slesinger, P. A. (2004) *J. Biol. Chem.* **279,** 28149–28158
35. Chakrapani, S., and Auerbach, A. (2005) *Proc. Natl. Acad. Sci. U. S. A.* **102,** 87–92
36. Halle, B. (2002) *Proc. Natl. Acad. Sci. U. S. A.* **99,** 1274–1279
37. Miller, C. (1989) *Neuron* **2,** 1195–1205

Spontaneous Thermal Motion of the $GABA_A$ Receptor M2 Channel-lining Segments

Amal K. Bera and Myles H. Akabas

J. Biol. Chem. 2005, 280:35506-35512.
doi: 10.1074/jbc.M504645200 originally published online August 9, 2005
